

Suyang Qin · Hong Liu · Yang Xiang

Lagrangian flow visualization of multiple co-axial co-rotating vortex rings

Received: 29 April 2017 / Revised: 29 August 2017 / Accepted: 31 August 2017 / Published online: 25 September 2017
© The Visualization Society of Japan 2017

Abstract This paper, for the first time, experimentally observes the detailed interacting phenomena of multiple co-axial co-rotating vortex rings using the method of finite-time Lyapunov exponent field. Besides the most attractive leapfrogging in dual vortex ring flows, several distinct phenomena are also found. The merger of squeezing is first observed in multiple vortex rings, resulting from the strong axial compressive induced effect. The inner vortex ring becomes axis-touching and cannot recover to the previous status. The merger due to elongation is already found in the previous studies. The inner vortex ring is elongated and distorted. The detachment of several independent vortex rings indicates that vortex merger has its limit, which is also a newfound phenomenon.

Keywords FTLE · Vortex ring · Leapfrogging · Merger

1 Introduction

Leapfrogging of a pair of co-axial co-rotating vortex rings, which is a fascinating vortex interacting phenomenon, has long been observed numerically and experimentally. Hicks (1922) gave analytical solution of the trajectories of two interacting rings. The slip-through motion of a vortex pair was simulated by Meleshko et al. (1992). After a theoretical description was first introduced (Helmholtz 1858), researchers have donated their efforts to present leapfrogging in laboratory experiments for several decades. After several failure (Maxworthy 1972; Oshima 1975), the successful leapfrogging in experiments was first reported by Yamada and Matsui (1978). It was later observed under different experimental conditions (Oshima 1978; Lim 1997). Due to mutual interaction, the radius of the front ring increases, while the rear one contracts radially. The front ring slows down and the rear one accelerates. Under favorable conditions, the rear ring catches up with the leading ring and slips through it. Thereafter, two vortex rings reverse their roles and the process repeats until they merge into a single vortex ring. It is difficult to observe leapfrogging, because the fluid is viscous and the ring core sizes are finite. In all the above-mentioned experiments of dual vortex rings, the vortex rings were visualized by smoke or dye. Further quantitative flow measurements, such as DPIV, were introduced to display the leapfrogging process (Mariani and Kontis 2010; Satti and Peng 2013). Vorticity fields were presented for flow visualization and characteristics of vortex rings were analyzed.

Electronic supplementary material The online version of this article (doi:10.1007/s12650-017-0450-6) contains supplementary material, which is available to authorized users.

S. Qin · H. Liu (✉) · Y. Xiang
J. C. Wu Center for Aerodynamics, School of Aeronautics and Astronautics, Shanghai Jiao Tong University, Shanghai 200240, People's Republic of China
E-mail: hongliu@sjtu.edu.cn

Although the leapfrogging of two vortex rings has been extensively investigated, cases involving more than two vortex rings have received a little attention. Recently, complex leapfrogging of three inviscid or viscous vortex rings was reported (Borisov et al. 2013, 2014). The results revealed that each of the vortex rings alternately slips through the other two rings ahead. The leapfrogging of viscous multiple vortex rings was simulated more specifically (Cheng et al. 2015). For more than two viscous vortex rings, the second ring slips through the leading one, followed by the third ring slipping through the other two ahead, which is contrary to the inviscid flow prediction. Experiments are necessary to entirely present the interacting process of multiple vortex rings, whereas no experimental result has been reported so far.

Regarding to the methods of flow visualization, the vorticity field is a traditional approach based on Eulerian perspective. The flows of multiple vortex rings are highly unsteady and complicated, so that Eulerian methods are of small use. An alternative to present the motion of multiple vortex rings is to study the wake from a Lagrangian perspective. Fluid particle trajectories are used as the fundamental variable. The proposal of finite-time Lyapunov exponent (FTLE) fields (Shadden et al. 2005; Haller 2015) is a new and better way to study the motion of multiple co-axial vortex rings. The FTLE fields is an objective diagnostic for Lagrangian coherent structures. Therefore, the present study aims to experimentally observe the detailed interacting phenomena of multiple co-axial co-rotating vortex rings using the method of FTLE field.

The present work experimentally visualizes the interacting phenomena of multiple co-axial co-rotating vortex rings by FTLE fields. The remainder of this paper is organized as follows. The experimental approach and FTLE method are described in Sect. 2. In Sect. 3, flow visualization of three and six successively generated vortex rings is presented with some discussion on the distinct phenomena. Finally, we conclude this paper in Sect. 4.

2 Experimental setup and method of flow visualization

2.1 Experimental setup

The experiments were conducted in a glass water tank (4 m L \times 1 m W \times 0.6 m H). Figure 1 shows the layout schematic of the features of the piston–cylinder apparatus. The nozzle was 5 cm in diameter and 50 cm in length. A wedge-shaped edge of 17° was used at the nozzle exit to promote clean vortex ring formation.

A CCD camera and a laser sheet were mounted to measure the flow on the symmetry plane using digital particle image velocity (DPIV). The flow was seeded with silver-coated neutrally buoyant hollow glass spheres with diameters in the range of 30–50 μm . The particles were illuminated with a 10-W Nd:YAG laser whose beam was formed into a 2-mm-thick sheet using a cylindrical lens. A CCD camera with a resolution of 2320×1200 pixels and a 50-Hz frame rate recorded the motion of particles. Particle movement was analyzed to determine the two-dimensional velocity vector of flow using a window shifting algorithm to cross-correlate the images with a 64×64 pixels correlation window size and a moving average step size of 16×16 pixels. The flow velocity vector fields were generated on 229×117 grids with a spatial resolution of 0.14×0.14 cm. It should be noticed that the measured plane was almost invariant in the flow regime considered because of the symmetries of the generated vortex rings. The surrounding flow in our experiments was quiescent. The only way to disturb the axisymmetric vortex rings was their mutual interaction. The raw PIV particle images, where particles travelled through the measured plane, were abandoned for velocity analysis, which showed that the vortex rings were totally disturbed.

The vortex rings were generated by several (three and six) successive pulses. As shown in Fig. 1, the piston velocity profile was constant acceleration and deceleration, and the maximum velocity was at the half of each pulse. The stroke length-to-nozzle diameter ratio L/D of each pulse was 1, and each pulse had a peak velocity of 10 cm s^{-1} . The jet Reynolds number is defined by the following:

$$Re = \frac{U_{\max} D}{\nu}, \quad (1)$$

where U_{\max} is the maximum piston velocity achieved during a jet pulse, D is the piston diameter, and ν is the kinematic viscosity. Based on the nozzle diameter and peak velocity, Reynolds number of each pulse was about 5000 in our experiments. Maxworthy (1972), Oshima (1978), and Yamada and Matsui (1978) proposed that successful leapfrogging will happen if Re is larger than 1600. Therefore, it is possible to observe leapfrogging in our experiments.

2.2 Finite-time Lyapunov exponent field

To visualize the flow structures, the distribution of the finite-time Lyapunov exponent (FTLE) field (Shadden et al. 2005, 2006; Haller 2001, 2015) was employed. A flow map $\phi_t^{t+T} : x(t) \rightarrow x(t+T)$ is defined as the mapping of a material point located at $x(t)$ at time t to its position $x(t+T)$ at time $t+T$ under the influence of fluid motion. The derivative of the flow map named deformation gradient is as follows:

$$\frac{d\phi_t^{t+T}(x)}{dx}. \quad (2)$$

Defining the finite-time Cauchy–Green deformation tensor as follows:

$$\Delta(x, t, T) = \left[\frac{d\phi_t^{t+T}(x)}{dx} \right]^T \frac{d\phi_t^{t+T}(x)}{dx}. \quad (3)$$

The FTLE measures the maximum stretching about a material point over a chosen time interval. It is defined as follows:

$$\sigma_t^T(x) = \frac{1}{|T|} \ln \sqrt{\lambda_{\max}(\Delta(x, t, T))}, \quad (4)$$

where $\lambda_{\max}(\Delta(x, t, T))$ denotes the maximum eigenvalue of $\Delta(x, t, T)$. The absolute value $|T|$ is used instead of T , because FTLE can be computed for $T > 0$ and $T < 0$. In the forward-time ($T > 0$) FTLE field, the strain rate normal to the ridge is positive (particle stretches away from the ridge). Conversely, in the backward-time ($T < 0$) FTLE field, the strain rate normal to the ridge is negative (particle attracts towards the ridge). Regions of maximum fluid particle separation ($T > 0$) and attraction ($T < 0$) produce local maximizing curves, which are “ridges” in FTLE field (Haller 2002).

The integration time $|T|$ is chosen according to the particular flow being analyzed. If a longer integration time is used, more of the boundary is revealed. In general, if the integration time $|T|$ is sufficiently long, the forward-time and backward-time FTLE ridges are more evident, and usually intersect to give the boundary of the vortex. As shown in Fig. 2, the FTLE ridges are fuzzy for $|T| = 1$ s. For $|T| = 3$ s and $|T| = 4$ s, however, the ridges are clear and long enough to give the boundary of the vortex rings. They are also similar to each other. Therefore, the maximum integration time for each case in our experiments is 3.00 s, which is sufficient to get the clear ridges of FTLE fields. In some cases, however, it is required that integration times

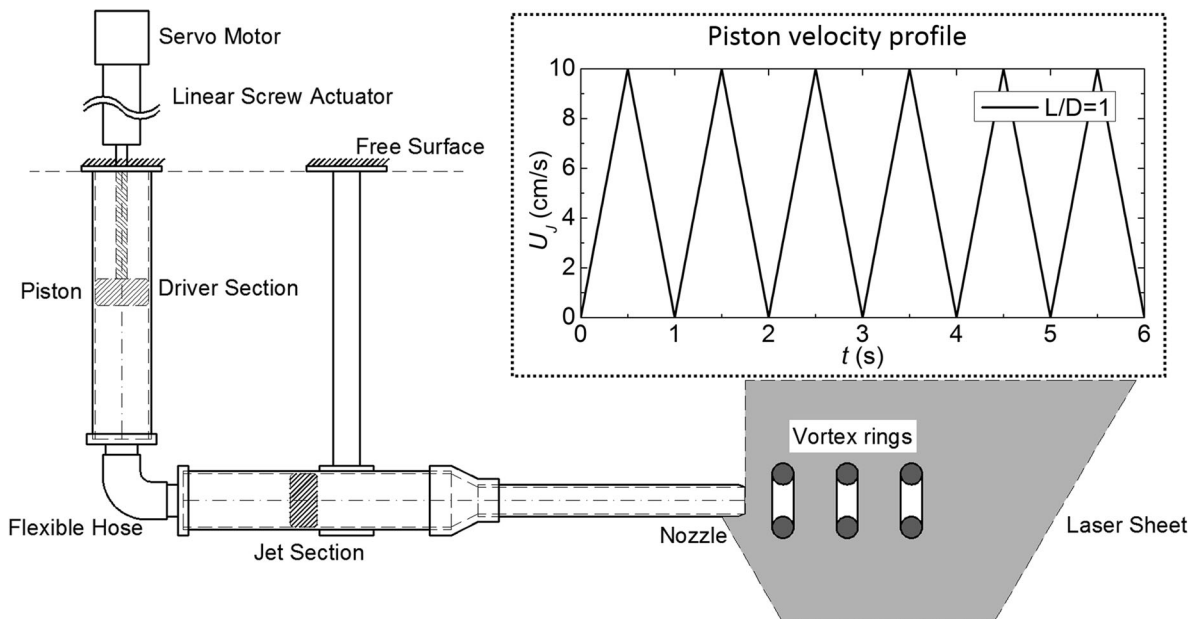


Fig. 1 Schematic view of the piston–cylinder apparatus and DPIV as well as the piston velocity profile

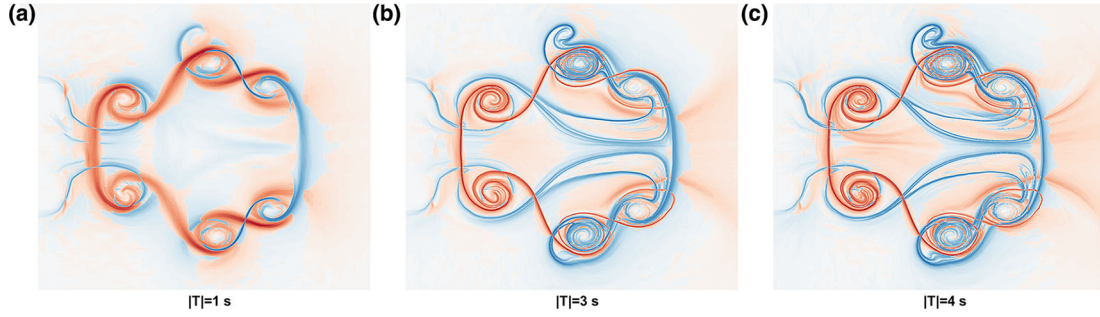


Fig. 2 Comparison of integration times for FTLE computation. The moment $t = 5.10$ s in three vortex rings is chosen

should be less than or equal to the piston movement time or the limiting frames of raw data. Integration time will be stated corresponding to every FTLE field.

Figure 3 shows the comparison of raw PIV particle image, velocity vectors, vorticity, and FTLE contours. It is hard to see the particle motion from only one PIV particle image. The velocity vectors are presented in Fig. 3a, which are the indicators of particle motion. Combining Fig. 3a, b, the centralized parts of FTLE ridges correspond to the vortex cores, and the outer FTLE ridges enclose all the vortex rings. The main flow characteristic is compared, which supports the accuracy of the FTLE method for flow visualization with respect to reality.

Figure 4 shows the comparison between Lagrangian and Eulerian methods for displaying vortex rings. Figure 4a–d presents the same instantaneous flow of a single vortex ring. Comparing Fig. 4a–d, the upper and lower intersections of forward-time and backward-time FTLE ridges perfectly match the corresponding zero magnitude of vorticity distribution along a line connecting cores of vortex rings, inside which is the region of the vortex ring. However, the Q -criteria and vorticity contours of a single vortex ring (Fig. 4b, c) can only roughly indicate the position of a vortex ring. Figure 4e–h shows the same instantaneous flow of dual vortex rings. Indicated from Fig. 4e, h, the intersections of forward-time and backward-time ridges between two vortex cores (indicated by red dots) correspond to the lowest value between two cores, which is the junction of the two cores, whereas the Euler methods cannot indicate such points. In addition, FTLE objectively shows the boundary of vortex, which Euler methods cannot do. Therefore, the FTLE method is a better choice for showing the motion of a vortex ring, even multiple vortex rings.

3 Results and discussion

3.1 Flow visualization of three vortex rings

Figure 5 shows the FTLE fields of the interacting process of three successively generated vortex rings. The number marked in the figure is the order of generation. Thus, we use “ V_n ” to represent the n th generated vortex ring. In addition, “ V_{nm} ” is the merged vortex ring of the n th and m th vortex rings.

A movie of three vortex rings is attached, which shows the evolution of FTLE and vorticity fields as real time increases. The characteristic moments are extracted from the movie and shown in Fig. 5. A complete successful leapfrogging process between V_1 and V_2 is presented from Fig. 5 a–f. At $t = 1.00$ s (Fig. 5a), the first stroke ends and V_1 has already formed. Due to the compressive induced effect of V_1 during formation, the vortex ring diameter of V_2 at its formation end is smaller than that of V_1 and also that of a single isolated ring, indicated by the black dotted lines in Fig. 5b. With the passing of time, the induced velocity of the leading vortex ring V_1 causes the rear ring V_2 to contract in diameter and accelerate. At the same time, the induced velocity of V_2 causes V_1 to expand and slow down (Fig. 5b, c). V_2 catches up with V_1 . As V_2 contracts to the condition that its diameter is just the same as or a little smaller than the inner path of V_1 , it is drawn through V_1 's center (Fig. 5c–e). Finally, the expanding V_2 appears ahead of the contracting V_1 and the two vortex rings reverse their roles.

In Fig. 5e, V_3 has already formed. Its diameter at the formation end is also smaller than that of a single isolated ring. Due to the induced effect, the diameter of V_3 contracts rapidly and it catches up with the leading two vortex rings. As shown from Fig. 5e–g, V_3 tries to go through V_1 , but fails in the end. The

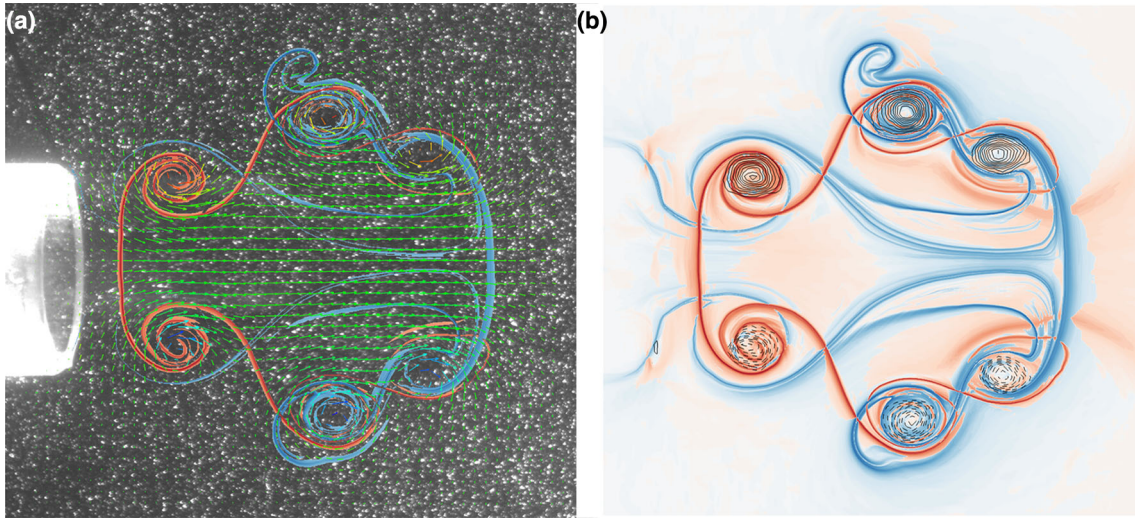


Fig. 3 Comparison of raw PIV particle image, velocity vectors, vorticity, and FTLE contours. The moment $t = 5.10$ s in three vortex rings is chosen. **a** Comparison of raw PIV particle image, velocity vectors, and FTLE ridges; **b** comparison of vorticity and FTLE contours. Black lines indicate vorticity. The integration times for FTLE fields are 3.00 s

contraction of a vortex ring has its limit. Indicated by the red dotted rectangle in Fig. 5f, g, the two inner ridges of backward-time FTLE lines near the symmetric axis of V3 are getting closer to each other when the ring is moving forward. In Fig. 5g, the upper and lower inner backward-time FTLE ridges touch together (in red rectangle), and then, the structure of V3 collapses due to the contraction of the outer vortex rings. V3 merges into V1 afterwards. V1 is strongly disturbed by the unsymmetrical V3 during this process, whereas the outer V2 is almost unaffected. The process of breaking down of axisymmetric vortex ring structure and finally merging into the outer ring is named as “merger of squeezing”. In the previous works, only Oshima (1975) seemed to observe the merger of squeezing by adjusting the relative jet velocity of the front and rear vortex rings. In dual vortex ring flows, the inner path of the front ring might be large enough for the rear ring to slip through or the compressive induced effect might not be strong enough to squeeze the rear ring. In numerical approaches (Cheng et al. 2015), the methods might not be able to simulate an unsymmetric structure or the relatively thin-core vortex rings are simulated.

The vorticity distributions along a line connecting two cores of vortex rings with the passing of time in Fig. 5 are shown in Fig. 6. Vorticity distribution reflects vortex core size related to vortex ring. For the leapfrogging process, the vorticity distributions of the leading V1 almost keep the same (Fig. 6a), whereas the rear V2 changes from initially thin core through relatively thick-core to finally thin-core vortex ring (Fig. 6b). During this process, ω/r of V2 does not reach the symmetry axis at the situation that vortex core is the thickest ($t = 4.20$ s). Indicated by the line of $t = 6.60$ s for V3 in Fig. 6c, the instantaneous symbol of merger of squeezing is that the inner vortex ring becomes axis-touching, i.e., ω/r extends to the symmetry axis, and cannot recover to its previous status.

3.2 Flow visualization of six vortex rings

More complicated flow structures exist in the FTLE fields of six successively generated vortex rings, as shown in Fig. 7. Here, the interacting phenomena for the leading three vortex rings are different from those introduced above, because V3 slows down because of the induced velocity of the rear rings. A movie of six vortex rings is attached, which shows the evolution of FTLE and vorticity fields as real time increases.

In Fig. 7a, V2 is elongated and warped by V1, and finally merges into V1 in Fig. 7b. Detailed FTLE fields of this process are shown in Fig. 8. V1 and V2 keep their own vortex structures in Fig. 8a, and later, V1 tries to warp V2. During this process, V2 is elongated and concurrently distorted (Fig. 8c–e), whereas V1 is little affected by the deformation of V2. Finally, V2 is merged into V1, and a new larger vortex ring V12 is formed and evolves with the passing of time (Fig. 8f). Such process is named as “merger of elongation”, which is distinct from the merger of squeezing. As shown in Fig. 7, the inner ridge of backward-time FTLE lines near the symmetric axis of V2 does not touch the axis of symmetry through all the moments. Merger of elongation is always observed in multiple vortex ring flows. It is also the final status of leapfrogging.

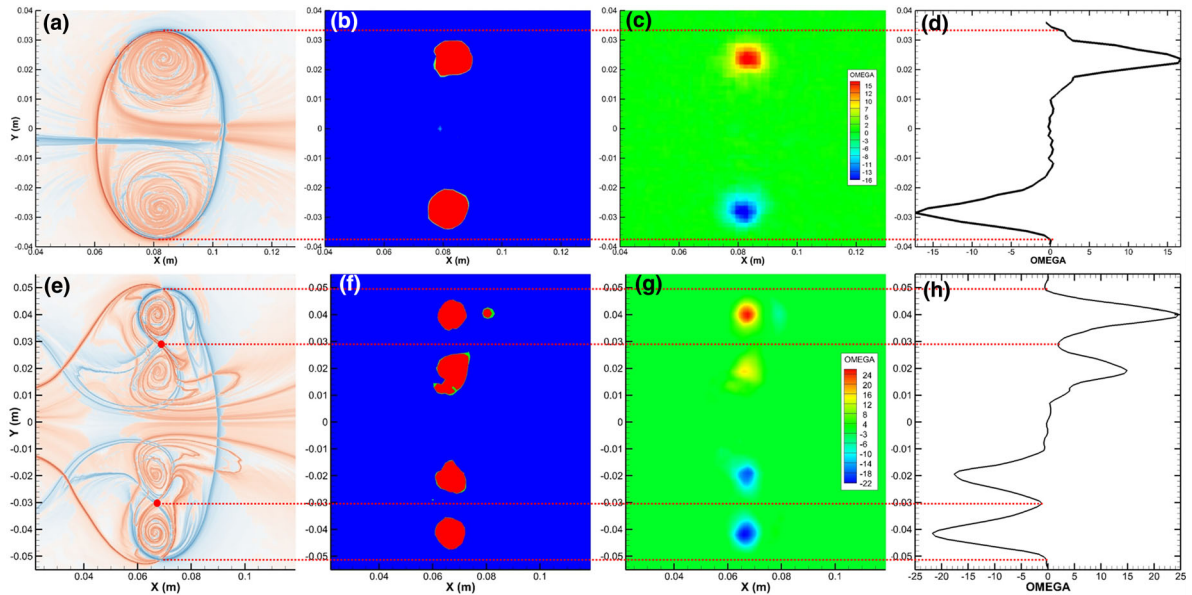


Fig. 4 Comparison between Lagrangian and Eulerian methods for displaying vortex rings. **a–d** Single vortex ring; **e–h** dual vortex rings. **a, e** Forward-time (red ridge line) and backward-time (blue ridge line) FTLE fields; **b, f** Q -criteria (Jeong and Hussain 1995) ($Q > 0$); **c, g** vorticity contour; **d, h** vorticity distribution along a line connecting cores of vortex. The integration times for FTLE fields are 3.00 s

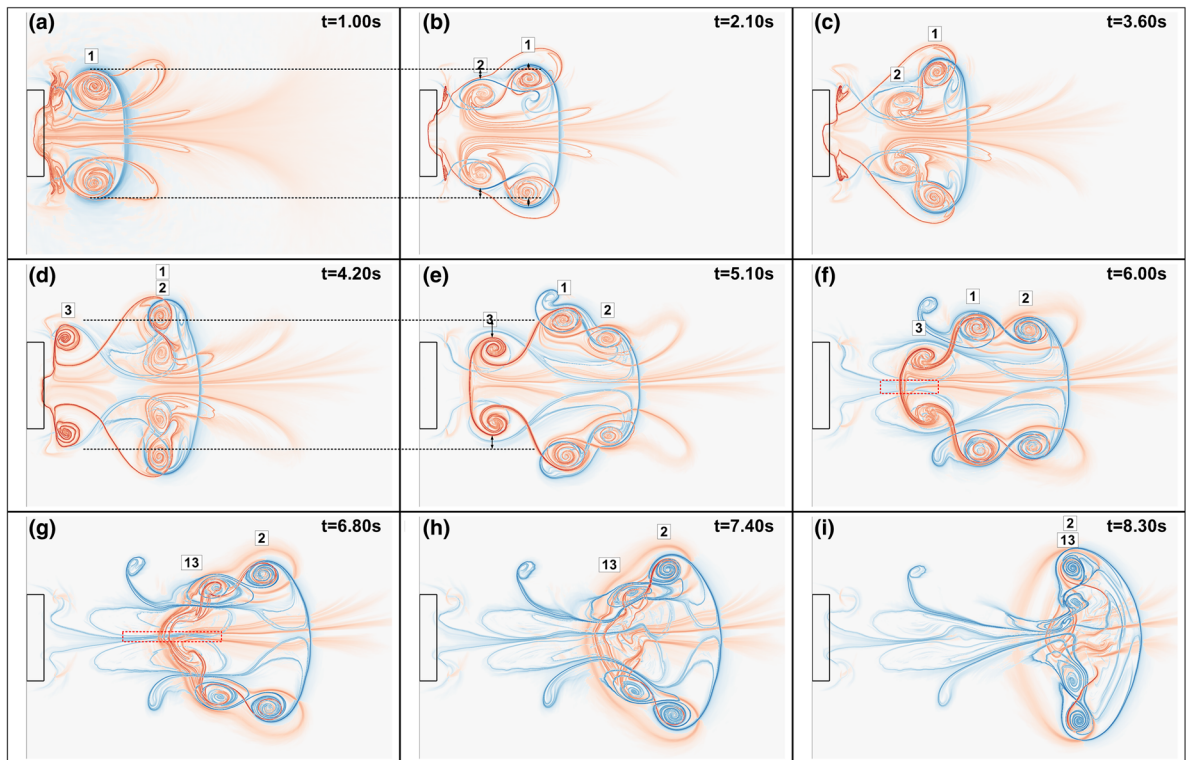


Fig. 5 FTLE fields of the interacting process of three successively generated vortex rings. The two black dotted lines indicate the vortex diameter of V1 at the formation end and also that of a single isolated ring. The black rectangle indicates the position and shape of nozzle. All the integration times are 3.00 s except that the backward-time integration times in panels **a** and **b** are 1.00 and 2.10 s, respectively, and forward-time integration times in panels **h** and **i** are 2.40 and 1.50 s, respectively

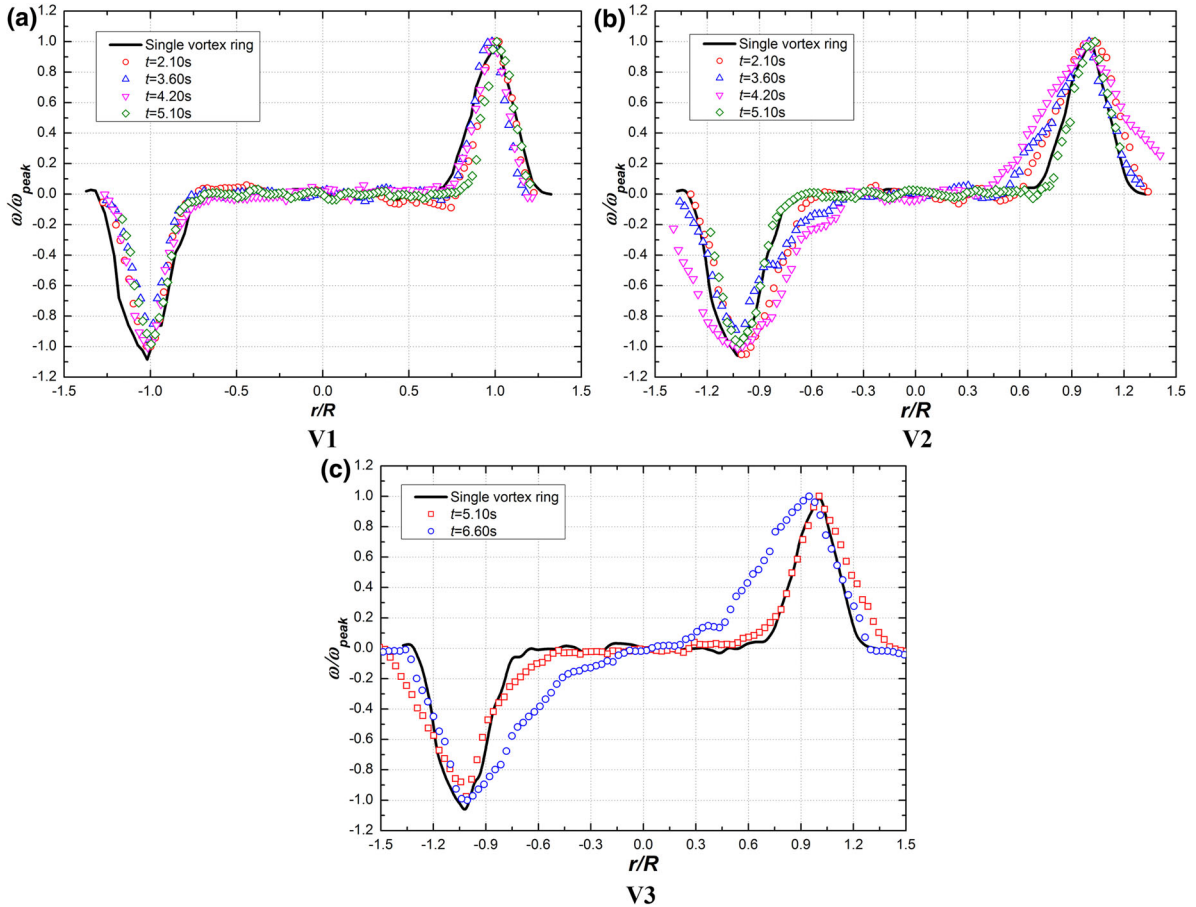


Fig. 6 Vorticity distributions along a line connecting two cores of vortex rings with the passing of time in Fig. 5. **a** V1; **b** V2; **c** V3

O’Farrell and Dabiri (2010) used forward-time FTLE to identify vortex pinch-off, which is the separation of the leading vortex ring and the trailing vortices. The intersection of forward-time FTLE between two vortex rings indicates the beginning of the merger, and the indistinguishable intersection of forward-time FTLE is indicative of the end of merger. It can be observed from Fig. 5b–f that the intersection of forward-time FTLE between V1 and V2 always exists during the leapfrogging process, which indicates the separation of V1 and V2. As shown in Fig. 8, however, the intersection between the vortices is distinguishable in Fig. 8a (indicated by red dotted line), whereas the forward-time FTLE of the two vortex rings becomes one line in Fig. 8b (indicated by red line). Although V2 still has its circulatory vortex structure shown by the backward-FTLE ridges, V2 has flux exchange with V1 from Fig. 8b. This can be a criterion based on visualization of forward-time FTLE fields, which is beyond the ability of Eulerian methods. In addition, further work should be conducted to investigate the elliptic LCSs denoted by coherent Lagrangian vortices (Haller 2015; Huhn et al. 2015) of these connected vortex rings to provide a mathematical criterion for merger. The latest Lagrangian vortex detection methods (Haller et al. 2016; Farazmanda and Haller 2016) provide potential ways to approach this criterion.

As shown from Fig. 7c, d, V4 and V5 merge into a new vortex ring V45. V45 does not catch up with the leading larger vortex ring V123. V6 is also an independent vortex ring. The independent evolution of V123, V45, and V6 in the wake is quite different from the numerical results of Cheng et al. (2015). In their study, the later vortex rings always slip through or merge into the leading rings, and only one vortex ring combining all the vortex rings is finally formed. In our experimental observation, the detachment of several independent vortex rings is found. In vortex formation, a vortex ring cannot grow infinitely, and it will finally reach the maximum circulation and pinch off from the trailing vortices (Gharib et al. 1998). In the meantime, it becomes axis-touching. Indicated from Figs. 5f and 6c, the inner backward-time FTLE ridges of a vortex ring become really close to each other, which indicates that the vortex ring is getting axis-

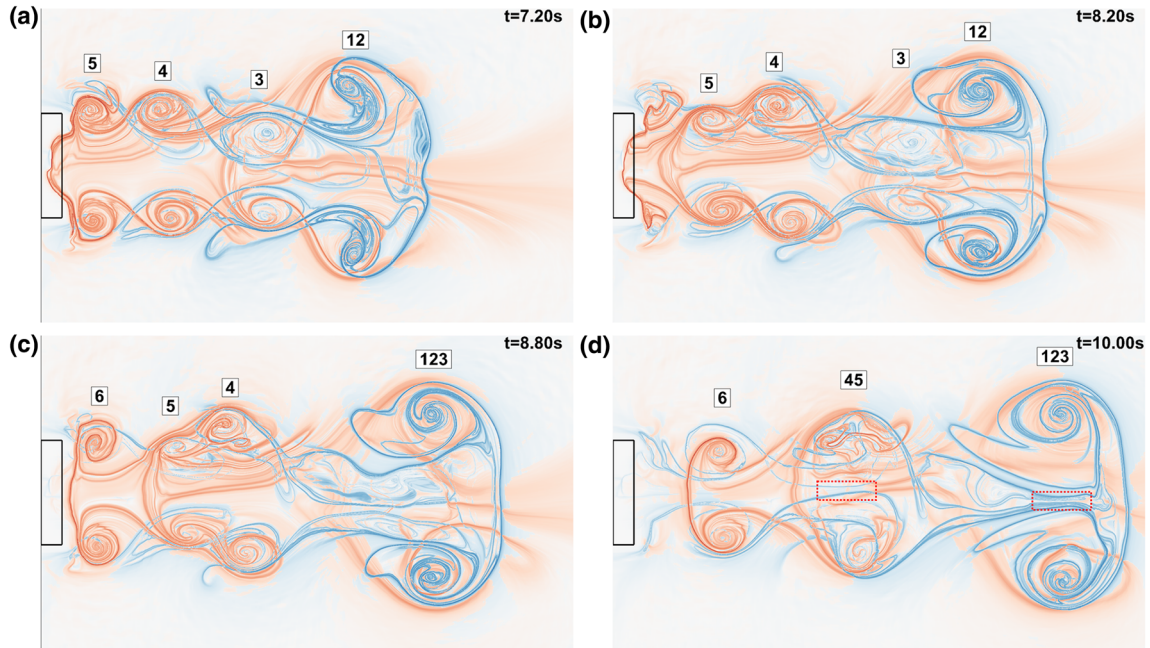


Fig. 7 FTLE fields of six successively generated vortex rings. The black rectangle indicates the position and shape of nozzle. All the integration times are 3.00 s except for the forward-time integration time in panel **d** is 2.00 s

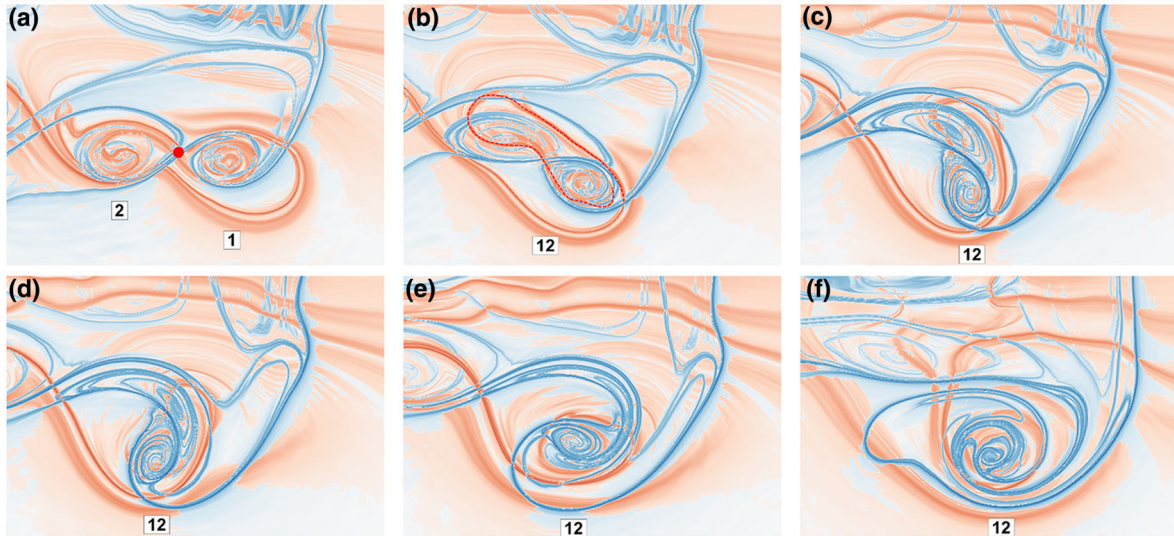


Fig. 8 Merging process due to vortex elongation shown by FTLE fields. All the integration times are 3.00 s

touching. As shown in Fig. 7d, therefore, V123 and V45 already reach their status that maintain the maximum circulation inside, and they will no longer merge other vortex rings. Thus, the detachment happens. However, in the simulation of Cheng et al. (2015), the initial core-to-radius ratio of a vortex ring is only 0.1, and the final single ring, which merges several rings, still does not reach the axis-touching status. It is indicated that this final vortex ring has the ability to merge other vortex rings.

4 Conclusion

This paper for the first time experimentally observes the detailed interacting phenomena of multiple co-axial co-rotating vortex rings using the method of FTLE field. Besides the most attractive leapfrogging of vortex rings, several distinct phenomena are also found. The merger of squeezing is first observed in multiple vortex rings, resulting from the stronger compressive induced effect compared with that in dual vortex flows. The structure of axisymmetric inner vortex ring breaks down and it finally merges into the outer ring. The instantaneous symbol of merger of squeezing is the axis-touching structure of the inner vortex ring. The other merger due to elongation is already found in the previous studies, which is also the final status of leapfrogging. The inner vortex ring is elongated and concurrently distorted by the outer ring. A criterion based on forward-time FTLE is used to distinguish the merged or un-merged vortices. The detachment of several independent vortex rings indicates that merger of vortex rings has its limit. If a vortex ring becomes axis-touching, it will not merge the vortex rings behind.

Acknowledgements Financial support from the State Key Development Program of Basic Research of China (2014CB744802) is gratefully acknowledged. Besides, this work was also supported by NSFC Project (91441205). The authors would also like to acknowledge the Center for High Performance Computing of Shanghai Jiao Tong University for providing the super computer- π to support this research.

References

- Borisov AV, Kilin AA, Mamaev IS (2013) The dynamics of vortex rings: leapfrogging, choreographies and the stability problem. *Regul Chaotic Dyn* 18:33
- Borisov AV, Kilin AA, Mamaev IS, Tenenev VA (2014) The dynamics of vortex rings: leapfrogging in an ideal and viscous fluid. *Fluid Dyn Res* 46(031):415
- Cheng M, Lou J, Lim TT (2015) Leapfrogging of multiple coaxial viscous vortex rings. *Phys Fluids* 27(031):702
- Farazmanda M, Haller G (2016) Polar rotation angle identifies elliptic islands in unsteady dynamical systems. *Physica D* 315:1–12
- Gharib M, Rambod E, Shariff K (1998) A universal time scale for vortex ring formation. *J Fluid Mech* 360:121–140
- Haller G (2001) Distinguished material surfaces and coherent structures in three-dimensional flows. *Physica D* 149:248–277
- Haller G (2002) Lagrangian coherent structures from approximate velocity data. *Phys Fluids* 14:1851–1861
- Haller G (2015) Lagrangian coherent structures. *Annu Rev Fluid Mech* 47:137–62
- Haller G, Hadjighasem A, Farazmand M, Huhn F (2016) Defining coherent vortices objectively from the vorticity. *J Fluid Mech* 795:136–173
- Helmholtz H (1858) Über integrale der hydrodynamischen gleichungen, welche den wirbelbewegungen entsprechen. *J Reine Angew Math* 1858:25–55
- Hicks WM (1922) On the mutual threading of vortex rings. *Proc R Soc Lond Ser A Contain Paper Math Phys Character* 102:111–131
- Huhn F, van Rees WM, Gazzola M, Rossinelli D, Haller G, Koumoutsakos P (2015) Quantitative flow analysis of swimming dynamics with coherent lagrangian vortices. *Chaos* 25(087):405
- Jeong J, Hussain F (1995) Optimal vortex formation as a unifying principle in biological propulsion. *J Fluid Mech* 285:69–94
- Lim TT (1997) A note on the leapfrogging between two coaxial vortex rings at low reynolds number. *Physica Fluids* 9:239–41
- Mariani R, Kontis K (2010) Experimental studies on coaxial vortex loops. *Phys Fluids* 22(126):102
- Maxworthy T (1972) The structure and stability of vortex rings. *J Fluid Mech* 51:15–32
- Meleshko VV, Konstantinov MY, Gurzhi AA, Konovaljuk TP (1992) Advection of a vortex pair atmosphere in a velocity field of point vortices. *Phys Fluids* 4:2779
- O'Farrell C, Dabiri JO (2010) A lagrangian approach to identifying vortex pinch-off. *Chaos* 20(017):513
- Oshima Y (1975) Interaction of two vortex rings moving along a common axis of symmetry. *J Phys Soc Jpn* 38:1159–66
- Oshima Y (1978) The game of passing-through of a pair of vortex rings. *J Phys Soc Jpn* 45:660–4
- Satti J, Peng J (2013) Leapfrogging of two thick-cored vortex rings. *Fluid Dyn Res* 45(035):503
- Shadden SC, Lekien F, Marsden JE (2005) Definition and properties of lagrangian coherent structures from finite-time lyapunov exponents in two-dimensional aperiodic flows. *Phys D* 212:271–304
- Shadden SC, Dabiri JO, Marsden JE (2006) Lagrangian analysis of fluid transport in empirical vortex ring flows. *Phys Fluids* 18(047):105
- Yamada H, Matsui T (1978) Preliminary study of mutual slip-through of a pair of vortices. *Phys Fluids* 21:292